EXHIBIT 26

RO-6-159

AGU PUBLICATIONS

Geophysical Research Letters

RESEARCH LETTER
10.1002/2015GL064924

Key Points:
- Warming since 1901 caused a significant trend toward drought in California
- Recent drought was naturally driven and modestly intensified by warming
- Warming has rapidly amplified the probability of severe drought

Supporting Information:
- Text S1, Table S1, and Figures S1–S7

Correspondence to:
A. P. Williams,
williams@ldeo.columbia.edu

Citation:
Williams, A. P., R. Seager, J. T. Abatzoglou, B. I. Cook, J. E. Smerdon, and E. R. Cook (2015), Contribution of anthropogenic warming to California drought during 2012–2014, *Geophys. Res. Lett.*, *42*, doi:10.1002/2015GL064924.

Received 11 JUN 2015
Accepted 1 AUG 2015
Accepted article online 20 AUG 2015

©2015. American Geophysical Union. All Rights Reserved.

Contribution of anthropogenic warming to California drought during 2012–2014

A. Park Williams[1], Richard Seager[1], John T. Abatzoglou[2], Benjamin I. Cook[1,3], Jason E. Smerdon[1], and Edward R. Cook[1]

[1]Lamont–Doherty Earth Observatory, Columbia University, Palisades, New York, USA, [2]Department of Geography, University of Idaho, Moscow, Idaho, USA, [3]NASA Goddard Institute for Space Studies, New York, USA

Abstract A suite of climate data sets and multiple representations of atmospheric moisture demand are used to calculate many estimates of the self-calibrated Palmer Drought Severity Index, a proxy for near-surface soil moisture, across California from 1901 to 2014 at high spatial resolution. Based on the ensemble of calculations, California drought conditions were record breaking in 2014, but probably not record breaking in 2012–2014, contrary to prior findings. Regionally, the 2012–2014 drought was record breaking in the agriculturally important southern Central Valley and highly populated coastal areas. Contributions of individual climate variables to recent drought are also examined, including the temperature component associated with anthropogenic warming. Precipitation is the primary driver of drought variability but anthropogenic warming is estimated to have accounted for 8–27% of the observed drought anomaly in 2012–2014 and 5–18% in 2014. Although natural variability dominates, anthropogenic warming has substantially increased the overall likelihood of extreme California droughts.

1. Introduction

During 2012–2014, drought in California (CA) caused water use restrictions, rapid drawdown of groundwater reserves [*Famiglietti*, 2014; *Harter and Dahlke*, 2014], fallowed agricultural fields [*Howitt et al.*, 2014], and ecological disturbances such as large wildfires and tree mortality [e.g., *Moore and Heath*, 2015; *Worland*, 2015]. The ultimate cause of the recent drought was a persistent ridge of high atmospheric pressure over the Northeast Pacific that blocked cold-season storms from reaching CA and stifled precipitation totals [e.g., *Seager et al.*, 2015]. Tree ring reconstructions from CA indicate that the resultant 3 year precipitation shortfall of 2012–2014 has been matched less than once per century over the past several hundred years [*Griffin and Anchukaitis*, 2014; *Diaz and Wahl*, 2015]. Dynamical studies agree that the Northeast Pacific ridge that caused the precipitation shortfall was part of an atmospheric wave train originating from the western tropical Pacific due to warm sea surface temperatures (SSTs) in that region [*Funk et al.*, 2014; *Seager et al.*, 2014a, 2015; *Wang and Schubert*, 2014; *Wang et al.*, 2014; *Hartmann*, 2015]. The observed ridging anomaly was stronger than the modeled response to tropical SST forcing [e.g., *Wang and Schubert*, 2014; *Seager et al.*, 2015], however, and leaves room for contributions from internal atmospheric variability or anthropogenic climate change. Although it has been suggested that anthropogenic emissions enhance the probability of *extreme* Northeast Pacific ridging events without necessarily affecting the long-term mean state [*Swain et al.*, 2014; *Wang et al.*, 2014, 2015], model projections of increased extremes in cold-season precipitation totals do not emerge as relevant until the second half of this century [*Berg and Hall*, 2015]. Furthermore, observed CA precipitation totals indicate no long-term trend despite cooccurring increases in western tropical Pacific SSTs [*Seager et al.*, 2015], climate models do not produce negative CA precipitation trends when forced by observed SST trends [*Funk et al.*, 2014], and future anthropogenic climate change is projected to result in slight *positive* trends in CA precipitation totals [*Neelin et al.*, 2013; *Seager et al.*, 2014b, 2015; *Simpson et al.*, 2015], all arguing against the likelihood of an anthropogenic role in the recent CA precipitation shortfall.

Importantly, there is widespread consensus that warmth has intensified the effects of the recent precipitation shortfall by enhancing potential evapotranspiration (PET) [*AghaKouchak et al.*, 2014; *Griffin and Anchukaitis*, 2014; *Diffenbaugh et al.*, 2015; *Mann and Gleick*, 2015; *Shukla et al.*, 2015]. Because warming is a well-understood and robustly modeled response to anthropogenic emissions of greenhouse gases, it is expected that warming-induced drying will continue for centuries to come [e.g., *Cook et al.*, 2015; *Diffenbaugh et al.*, 2015]. However, the degree to which anthropogenic warming and resultant increases in PET were responsible for the recent drought severity in CA is unknown.

Griffin and Anchukaitis [2014] used the Palmer Drought Severity Index (PDSI), a proxy for near-surface soil moisture [*Palmer*, 1965], to investigate the role of temperature in the recent drought, but they did not separate the influence of anthropogenic warming from natural temperature variability and their employed version of PDSI (from the National Oceanic and Atmospheric Administration (NOAA)) uses a simplified formulation of PET. *Mao et al*. [2015] attempted to isolate the anthropogenic component of warming using a more physically based PET calculation but focused only on the Sierra Nevada Mountain region and spring snowpack, and simply characterized anthropogenic warming as the observed linear trend in daily minimum temperatures. Other studies investigate the effect of warming on the likelihood of severe drought events in CA [e.g., *AghaKouchak et al*., 2014; *Diffenbaugh et al*., 2015; *Shukla et al*., 2015] but do not directly address the anthropogenic contribution to recent drought severity. Each study noted above considers only a single climate data product without addressing the structural uncertainty across different data products.

Here we quantify the severity of recent CA drought using an ensemble of data products and multiple PDSI formulations, determine the relative roles of individual components of the water balance, and determine the proportion of recent drought severity that can be attributed to increases in PET due to anthropogenic warming.

2. Methods

2.1. Palmer Drought Severity Index

We calculate monthly PDSI to characterize temporal and spatial variations in CA drought from 1901 to 2014: most humidity, wind speed, and insolation data sets do not extend prior to 1901. The PDSI is based on a simple two-layer soil moisture model and is locally normalized to reflect moisture anomalies relative to long-term mean conditions. PDSI is a primary tool used for drought monitoring in the United States [*Heim*, 2002; *Svoboda et al*., 2002] and generally agrees well with modeled and observed soil moisture anomalies [*Dai et al*., 2004; *Cook et al*., 2015; *Smerdon et al*., 2015; *Zhao and Dai*, 2015] and tree ring records [*Cook et al*., 2007]. While some recent studies have taken more complex modeling approaches to investigate the recent CA drought [*Mao et al*., 2015; *Shukla et al*., 2015], we use the PDSI because it allows efficient calculations of centennial-length records at high spatial resolution, which can be computed many hundreds of times with different climate variables, input data sets, and methodological schemes. The PDSI only reflects drought variability from a climatological perspective. Our results therefore do not explicitly reflect human water demand, stream flow and reservoir storage, or accessibility of groundwater. The PDSI also considers all precipitation to occur as rain, neglecting snow storage and subsequently delayed inputs to soil moisture and runoff. To assess implications of this latter simplification, PDSI is compared to modeled soil moisture by *Mao et al*. [2015] for the snow-dominated Sierra Nevada mountains.

Other studies also have used the PDSI to examine recent CA drought [*Griffin and Anchukaitis*, 2014; *Diffenbaugh et al*., 2015; *Robeson*, 2015]. A key difference between these studies, which use data developed by NOAA, and our study is the formulation of PET. The NOAA calculations involve the simplified Thornthwaite formula [*Thornthwaite*, 1948] that considers monthly mean temperature to be the only climatological driver of PET variability. This approach can overemphasize the influence of warmth when temperatures are high, and further inaccuracies are introduced by ignoring the nontemperature components of PET [e.g., *Hobbins et al*., 2008; *Hoerling et al*., 2012; *Sheffield et al*., 2012]. The more physically based Penman-Monteith (PM) formula [*Penman*, 1948; *Monteith*, 1965] considers the suite of variables affecting PET: mean daily maximum temperature (T_{max}), mean daily minimum temperature (T_{min}), humidity, wind speed, and net radiation. We use the PM formula and repeat calculations using Thornthwaite in some cases for comparison. Additionally, we use the newer self-calibrated PDSI ($PDSI_{sc}$), developed to make drought severity comparable among locations [*Wells et al*., 2004].

Consistent with several prior studies [e.g., *Cook et al*., 2004, 2007, 2010; *Griffin and Anchukaitis*, 2014], we focus on June–August (JJA). $PDSI_{sc}$ is an integration of hydroclimate over multiple months to several years [*Guttman*, 1998] and summer is the ideal season for characterizing drought intensity in CA for two reasons: (1) it is when drought effects tend to be most critical; and (2) it is when $PDSI_{sc}$ is most accurate in mountain regions because snowpack has melted or is at a minimum [e.g., *Dai et al*., 2004]. To facilitate interpretation, each grid cell's annual record of JJA $PDSI_{sc}$ is normalized so that two $PDSI_{sc}$ units equal a 1 standard deviation departure from the 1931–1990 mean, retaining a similar variance in the records of JJA $PDSI_{sc}$ as is in the

monthly records. Again for interpretability, we renormalize statewide mean JJA $PDSI_{sc}$ records. We use a 1931–1990 calibration interval in all $PDSI_{sc}$ calculations to be consistent with NOAA methodology.

2.2. Climate Data

We calculate $PDSI_{sc}$ records for all 432 combinations of four precipitation, four temperature, three vapor pressure, three wind speed, and three insolation data sets. Data sets are listed with references in Table S1 in the supporting information and described in Text S1. We bilinearly interpolate each monthly climate field for each data set to the spatial resolution of the PRISM data set (0.04167°) [*Daly et al*., 2004]. For each climate variable, data sets were calibrated so that climatological means and variances match during 1961–2010 (see Text S1). Uncertainties are high for humidity, wind speed, and insolation because they are largely based on models or observations of other variables [e.g., *Dai*, 2011]. Although consideration of multiple data products helps to characterize some of this uncertainty, data products are not all produced independently. Errors therefore may be recurrent in multiple data products (see Text S1).

2.3. Decomposition of PET and $PDSI_{sc}$

We calculate the influence of a given variable, or subset of variables, on PET as the PET anomaly calculated while holding all other variables at their mean annual cycles [e.g., *Cook et al*., 2014; *Scheff and Frierson*, 2014; *Zhao and Dai*, 2015]. Mean annual cycles were always defined over 1961–2010. For $PDSI_{sc}$, the contribution of precipitation was defined as $PDSI_{sc_P}$, calculated by holding PET at its mean annual cycle and only allowing precipitation to vary. The contribution of PET was calculated as the difference between $PDSI_{sc_P}$ and a recalculation of $PDSI_{sc}$ in which both precipitation and PET vary. We isolated the influences of the temperature and nontemperature components of PET by applying versions of PET in which only the component of interest varies. Contributions of subcomponents of PET and $PDSI_{sc}$ anomalies were nearly perfectly additive, but all relative anomalies were rescaled to sum to exactly 100% of the total anomaly.

2.4. Effect of Anthropogenic Warming

Anthropogenic warming was isolated from that of natural temperature variability by considering four warming scenarios that are described in detail in the next two paragraphs. For each scenario, natural temperature variability is calculated as the observed temperature minus the anthropogenic trend. All records of anthropogenic warming and natural variability were calculated independently for T_{max} and T_{min}, each grid cell, and each month. For each warming scenario, we recalculated PET twice: once considering only the anthropogenic warming record and once considering the residual record of natural temperature variability. Methods were repeated from above to assess $PDSI_{sc}$ anomalies caused by anthropogenic warming and natural temperature variability.

The four anthropogenic warming scenarios are defined as follows: (1) linear trend, (2) 50 year low-pass filter (using a 10-point butterworth filter), (3) unadjusted mean trend from an ensemble of climate models, and (4) an adjusted version of #3. The first two warming scenarios represent empirical fits to the observed temperature records during 1895–2014. Although a linear trend is commonly used to represent the anthropogenic effect, a linear fit to a centennial temperature record may underestimate the human effect on temperature in recent decades because radiative forcing during this period has increased relatively rapidly [e.g., *Myhre et al*., 2013]. The 50 year low-pass filter partially addresses this issue, but multidecadal natural temperature variability inhibits complete isolation of the anthropogenic effect with either the linear trend or the 50 year filter. Additionally, trends toward the end of the 50 year filter record are affected by boundary constraint assumptions. Although continued warming is likely, we pad the end of the temperature record with a repetition of the last 25 years in reverse order, likely leading to an underestimation of anthropogenic warming in the most recent years.

In the third and fourth warming scenarios, we use modeled records of T_{min} and T_{max} produced for the Coupled Model Intercomparison Project Phase 5 (CMIP5) [*Taylor et al*., 2012] to represent anthropogenic warming trends for each month. Thirty-six models in the CMIP5 archive are used, based on the availability of T_{max} and T_{min} data for the historical (1850–2005) and future (2006–2099, RCP 8.5 [*van Vuuren et al*., 2011]) simulations. For each model, T_{min} and T_{max} are each averaged across all available runs for the historical and future periods, bilinearly interpolated to the geographic resolution of PRISM, and bias corrected for each grid cell so that monthly means during 1961–2010 matched observational means. We calculate 50 year low-pass filtered time series for each month during 1850–2099 and average across the 36 models. The resultant ensemble mean records for 1895–2014 represent the CMIP5 records of anthropogenic warming used in the

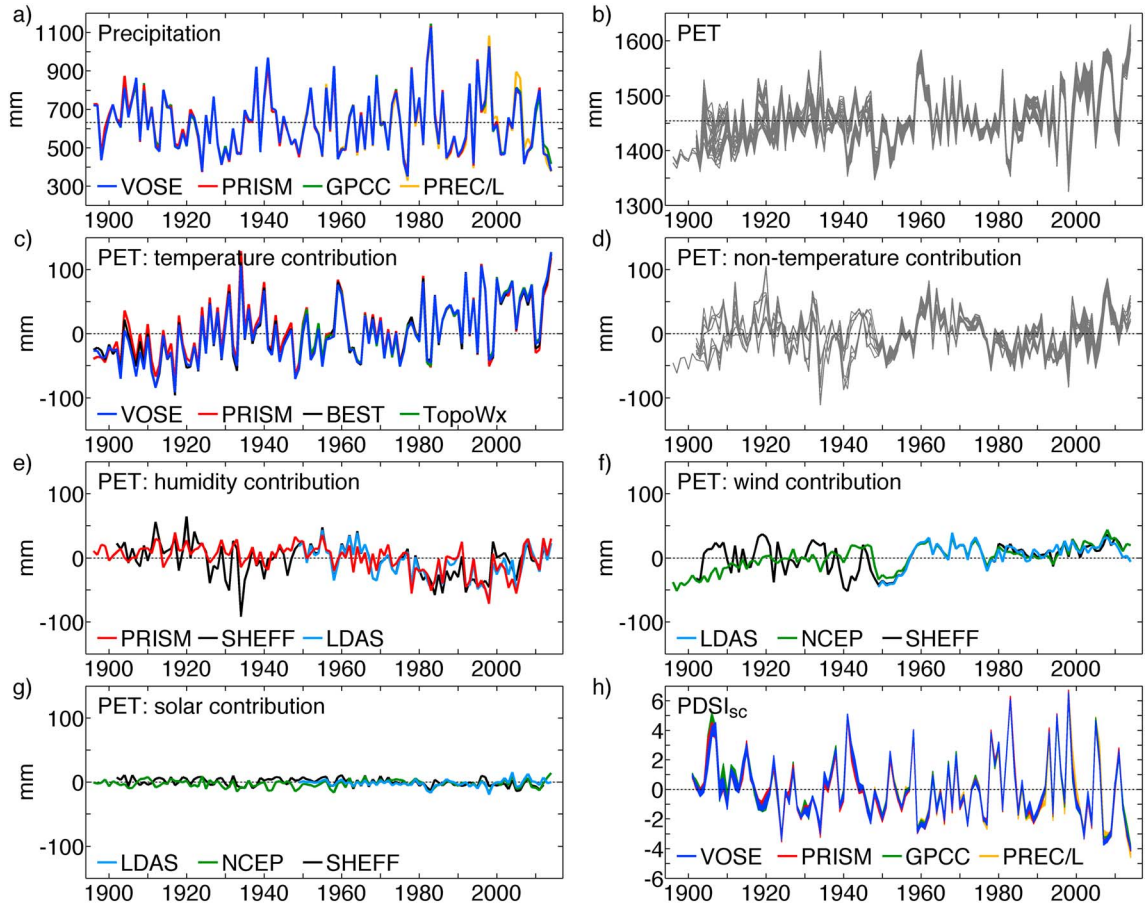

Figure 1. Contributors to interannual (water year) drought variability in CA, calculated from multiple data sets. (a) Precipitation. (b) PET totals, calculated using the PM equation for all combinations of four temperature, three humidity, three wind velocity, and three insolation data sets. (c) Temperature contribution to PET anomalies. Contributions of (d) all nontemperature variables, (e) humidity, (f) wind velocity, and (g) insolation to PET anomalies. (h) JJA $PDSI_{SC}$ calculated with all 432 combinations of the climate-variable data sets. Horizontal black lines: 1931–1990 means. Colors distinguish data products.

third warming scenario. For the fourth scenario, we linearly adjust these records to best fit the observations from 1895 to 2014. This approach reduces biases in the modeled trends but carries the implicit assumption that observed temperature trends are entirely anthropogenic in origin, which is a questionable assumption. For example, *Johnstone and Mantua* [2014a] indicate that some of the observed warming trend may be due to warming in the Northeast Pacific that is not linked to anthropogenic climate change, but also see *Abatzoglou et al*. [2014] and *Johnstone and Mantua* [2014b].

3. Results and Discussion

3.1. Recent Drought Conditions

Figure 1a shows annual water year (WY: October–September) CA precipitation totals for 1896–2014 and demonstrates general agreement among the four gridded data sets. The WY 2014 precipitation total was the third lowest (fourth lowest for Global Precipitation Climatology Centre (GPCC) [*Schneider et al*., 2014]) on record (behind WYs 1977 and 1924) and WY 2012–2014 precipitation was the lowest (third lowest for GPCC) 3 year running average on record (Figure S1a). The effects of the recent precipitation deficit have been amplified by positive PET anomalies. Figure 1b shows the 108 records of WY PET, calculated from all combinations of temperature, humidity, wind, and insolation data sets. Among the PET records, 32 include data for 2014. WY 2014 PET was 9–12% above average and the highest on record in every case. PET for WY 2012–2014 was 7–9% above average and either the highest or second highest (behind WY 2007–2009) on record (Figure S1b).

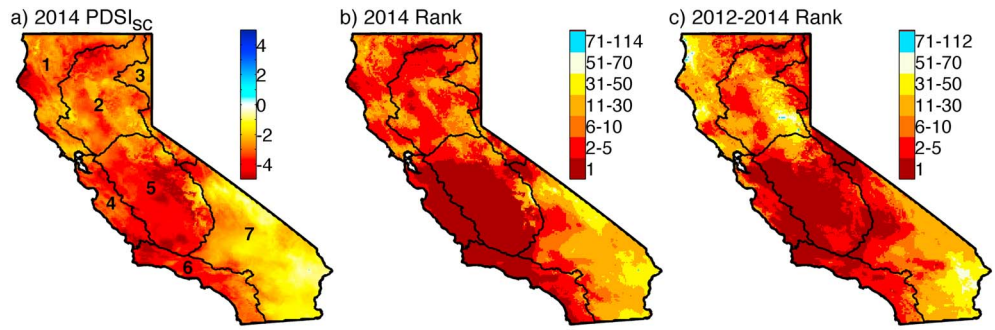

Figure 2. Maps of (a) JJA PDSI$_{sc}$ and ranking for (b) 2014 and (c) 2012–2014. Rankings are based on all years between 1901 and 2014, and a ranking of 1 indicates record-breaking drought. PDSI$_{sc}$ in this figure is based on VOSE precipitation and temperature, PRISM humidity, and LDAS [*Mitchell et al.*, 2004; *Rodell et al.*, 2004] wind speed and insolation. Polygons bound the seven NOAA climate divisions (division numbers shown in Figure 2a).

All PET data sets indicate positive and significant trends during WY 1949–2014, ranging from 8.2 to 13.7 mm/decade when considering linear trends. These trends are almost entirely due to warming. Since WY 1949, warming positively forced PET by 10–12 mm/decade (65–82 mm total), equivalent to 10–13% of the mean WY precipitation (Figure 1c). The VOSE [*Vose et al.*, 2014], BEST [*Rohde et al.*, 2013], and TopoWx (which only goes back to 1948 [*Oyler et al.*, 2015]) data sets indicate that the temperature contribution to PET was highest on record in 2014 while PRISM indicates that the temperature contribution was higher in 1934. All four data sets agree that the temperature contribution to PET during WY 2012–2014 was substantially higher than that of any other 3 year period on record (Figure S1c).

Nontemperature variables account for approximately one third of WY PET variability (Figure 1d), although much uncertainty exists among the nontemperature data sets. Nearly all interannual variability and inter–data set spread in nontemperature PET (Figure 1d) are due to contributions from vapor pressure and wind speed (Figures 1e–1g). According to the data sets considered, positive wind speed trends contributed positively to PET (4.5 to 4.8 mm/dec), positive humidity trends contributed negatively (−3.5 to −4.0 mm/dec), and insolation had a minimal influence due to very low interannual variability in warm-season insolation relative to the mean. Prior to 1948, trends in the nontemperature components of PET are much less certain due to a nearly complete lack of pre-1948 observational data [e.g., *Dai*, 2011].

Within CA, PET trends were spatially heterogeneous, with much of the Central Valley experiencing reduced PET during the second half of the twentieth century due to suppressed daytime warming and increased humidity, consistent with the effects of increased irrigation [*Lobell and Bonfils*, 2008]. These results are broadly consistent with observed decreases in warm-season pan evaporation at sites in the Central Valley during 1951–2002 [*Hobbins et al.*, 2004]. These agricultural trends appear distinct from the well-known global declines in pan evaporation that appear to have been caused by pollution-induced solar dimming during the 1950s–1980s and reductions in wind speed [*Roderick et al.*, 2009]. While long-term records of insolation and wind speed are sparse in CA, those that exist indicate insignificant wind trends of inconsistent sign [*Pryor et al.*, 2009; *Pryor and Ledolter*, 2010] and twentieth century insolation decreases that were too small to substantially affect statewide mean PET, similar to prior findings in Australia [*Roderick et al.*, 2007].

Figure 1h shows all 432 records of JJA PDSI$_{sc}$ for 1901–2014 (128 records extend through 2014). Colors in Figure 1h indicate the precipitation product; spread among colors reflects disagreement among precipitation products and spread within colors reflects disagreement among PET products. All records indicate that 2014 JJA PDSI$_{sc}$ was the lowest on record (−4.64 to −3.67), with 25–37% of CA experiencing record-breaking drought locally. The year 2014 had the highest proportion of record-breaking drought area on record for all data sets, with the most severe anomalies centered in the southern Central Valley and the central and southern CA coasts (Figures 2a and 2b).

Considering 3 year running average PDSI$_{sc}$, 2012–2014 JJA drought intensity was found to be similar to, but generally not as severe as, that of 2007–2009 when averaged across CA, regardless of data sets used (Figure S1h). The similarity of mean PDSI$_{sc}$ during these two periods is interesting given that WY 2012–2014 had the lowest precipitation total on record and PET levels were comparable during each period. The difference

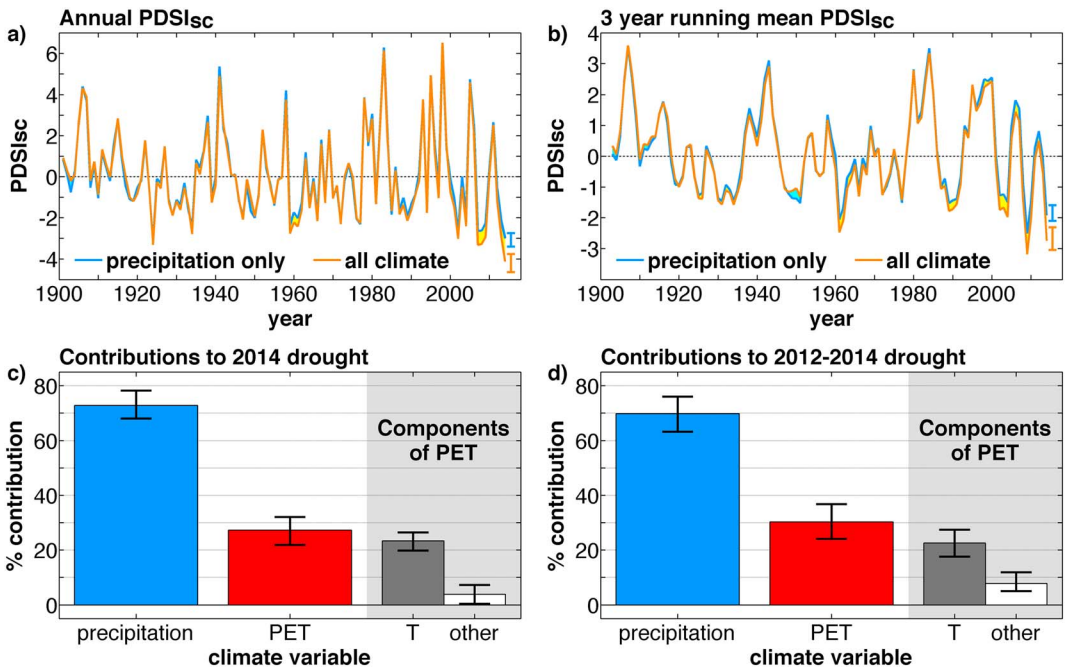

Figure 3. Contributions of precipitation and PET to drought variability. (a) Annual and (b) 3 year running mean JJA $PDSI_{sc}$ records calculated when (blue) only precipitation is allowed to vary from the climatological mean and (orange) when both precipitation and PET vary. Thus, departures of the blue line from zero are due to precipitation variability and departures of the orange line from the blue line are due to PET variability. Shading between lines in Figures 3a and 3b indicate periods when (cyan) low PET reduces drought and (yellow) high PET intensifies drought. Percent contributions of precipitation and PET to the (c) 2014 and (d) 2012–2014 $PDSI_{sc}$ anomalies. The bars in the shaded area of Figures 3c and 3d break the contribution of PET into contributions from temperature (*T*) and nontemperature (other: humidity, wind, and solar). Time series and bars represent mean conditions across all combinations of climate data products and whiskers bound all values from all combinations of data products.

was in the timing of precipitation. Unlike the 2012–2014 drought, which intensified over time, the 2007–2009 drought was most intense at the onset and the moisture deficit established in 2007 partially propagated into 2008 and 2009. Additionally, spring months for WY 2012-2014 were generally wetter than WY 2007–2009, contributing to soil moisture at a critical time immediately prior to summer (Figure S2).

The finding that the 2012–2014 $PDSI_{sc}$ was not as severe as that of 2007–2009 conflicts with prior findings based on NOAA PDSI (which is based on VOSE precipitation and temperature) that 2012–2014 was the most severe 3 year drought on record in CA [*Griffin and Anchukaitis*, 2014; *Robeson*, 2015]. This is attributable to the NOAA calculation of PDSI, which amplifies the effect of extreme heat anomalies in 2014 via the Thornthwaite PET equation (Figures S3 and S4). Importantly, while our calculations indicate that 2012–2014 was probably not a record-breaking drought event when averaged across CA, 2012–2014 drought severity *was* record breaking in much of the agriculturally important Central Valley (Figure 2c). In contrast, drought in 2007–2009 was most severe in the sparsely populated and already dry desert region of southeastern CA.

$PDSI_{sc}$ does not account for snowpack effects, which are important for human water supply, and our calculations of statewide $PDSI_{sc}$ may therefore not always accurately reflect drought from the perspective of human water supply, which is disproportionately linked to the Sierra Nevada Mountains. For that region, *Mao et al.* [2015] used the Variable Infiltration Capacity (VIC) hydrologic model [*Liang et al.*, 1994] to simulate hydrological dynamics during 1920–2014. Using the *Mao et al.* [2015] meteorological forcing to calculate $PDSI_{sc}$ for the Sierra Nevada Mountains, we find strong agreement ($r = 0.93$) with VIC JJA soil moisture (Figure S5). VIC soil moisture nevertheless indicates slightly more severe drought than $PDSI_{sc}$ during the most extreme drought years, likely due to early disappearance of snowpack [e.g., *Mote*, 2006; *Mankin and Diffenbaugh*, 2015] and subsequently reduced spring and summer melt-driven soil moisture inputs (Figure S6). Given that the calculation of $PDSI_{sc}$ neglects snowpack and therefore cannot capture the effect of early snowmelt on summer soil moisture, the warming effect on summer $PDSI_{sc}$ presented in the next section is likely conservative for snow-dominated areas.

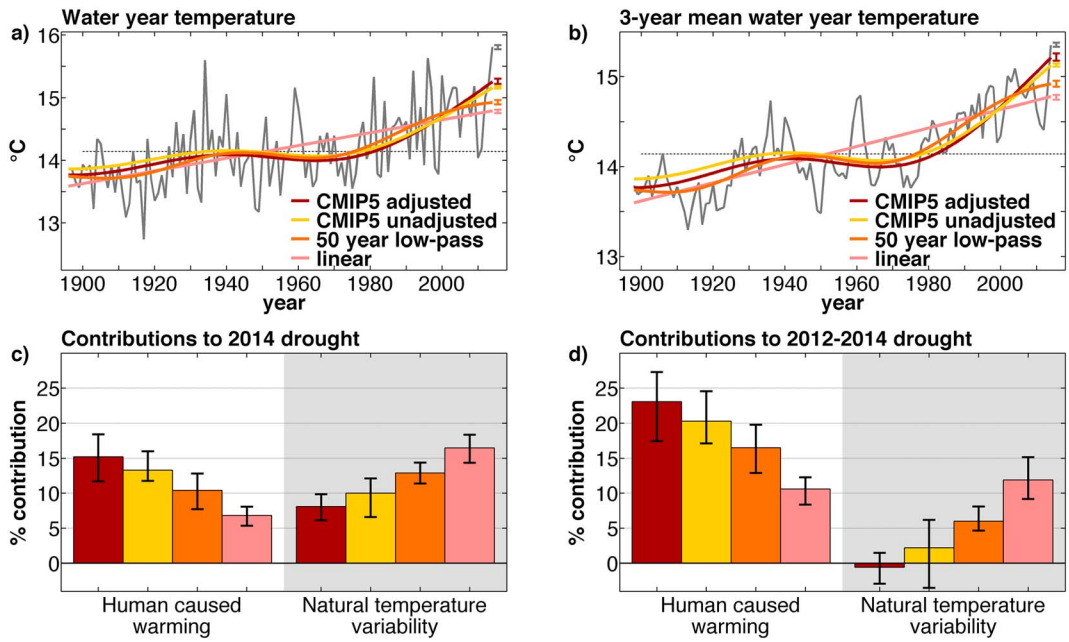

Figure 4. Contributions of anthropogenic warming and natural temperature variability to recent temperature and drought. (a) Annual and (b) 3 year running water year temperature records with four alternate scenarios of anthropogenic warming. Contributions of anthropogenic warming versus natural temperature variability to (c) 2014 and (d) 2012–2014 JJA $PDSI_{sc}$ anomalies, where bar colors correspond to the colors of the four anthropogenic warming trends in Figures 4a and 4b. For each of the anthropogenic warming scenarios, natural temperature variability is calculated as the observed temperature minus the warming trend. All time series and bars represent mean conditions across all combinations of climate products. Whiskers bound all values for all combinations of data products.

3.2. Effect of Warming on Recent Drought

Figures 3a and 3b compare $PDSI_{sc}$ (orange) to an alternate calculation in which only precipitation varies and PET is held at its mean annual cycle (blue). While there is no long-term trend in precipitation-driven $PDSI_{sc}$ since 1948 or 1901, trends in actual $PDSI_{sc}$ are significant and negative ($p < 0.05$ according to Spearman's Rho and Kendall's Tau) due to increasing PET. During 2014 and 2012–2014, PET anomalies accounted for 22–32% and 24–37% of the JJA $PDSI_{sc}$ anomalies, respectively (Figures 3c and 3d). Recalculating $PDSI_{sc}$ considering the temperature and nontemperature components of PET separately, we find that the intensifying effect of high PET on recent drought was nearly entirely caused by warmth (Figures 3c and 3d). High temperatures accounted for 20–26% and 18–27% of the JJA $PDSI_{sc}$ anomalies in 2014 and 2012–2014, respectively (Figures 3c and 3d).

The contribution of temperature is further separated into contributions from natural temperature variability and anthropogenic warming in Figure 4. Figures 4a and 4b show the WY temperature record and the four anthropogenic warming scenarios, which indicate an anthropogenic warming contribution in WY 2014 of 0.61–1.27°C relative to the 1931–1990 mean. The empirically derived trends suggest a weaker anthropogenic warming contribution in recent years than the CMIP5 trends because (1) the linear trend does not account for the nonlinear increase in anthropogenic forcing and (2) the 50 year low-pass filter trend indicates slowed warming in the past two decades that is partly due to our conservative smoothing approach and partly due to decadal climate variability. The CMIP5 trends represent the nonlinear increase in radiative forcing without being affected by decadal climate variability or smoothing artifacts. The similarity between the adjusted and unadjusted CMIP5 warming trends suggest that the CMIP5 provides a reasonable representation of the anthropogenic warming influence in CA despite having stronger warming trends than the conservatively designed empirical trends.

Breaking the temperature contributions to $PDSI_{sc}$ into anthropogenic and natural components, the four anthropogenic warming trends account for 5–18% of the JJA $PDSI_{sc}$ anomaly in 2014 and 8–27% of the anomaly in 2012–2014 (Figures 4c and 4d). Despite differences in these relative contributions of warming

to drought during 2014 versus 2012–2014, the *absolute* contributions of anthropogenic warming to drought during these two periods were virtually identical. The absolute anthropogenic contribution does not change much interannually but instead acts as a gradually moving drought baseline upon which the effects of natural climate variability are superimposed (Figure S7a).

As of 2014, the anthropogenic warming forcing accounted for approximately −0.3 to −0.7 standardized $PDSI_{sc}$ units, depending on the anthropogenic warming scenario and combination of climate data sets considered (Figure S7a). To illustrate how this trend in background drought conditions affected the probability of severe drought as of 2014, we compare the probability distribution of 1901–2014 $PDSI_{sc}$ values calculated in the absence of anthropogenic warming to the same distributions shifted negative by 0.46, the 2014 $PDSI_{sc}$ forcing by the 50 year low-pass filter warming trend (Figure S7b, based on VOSE temperature and precipitation data). Comparing the two distributions, we find that severe summer droughts with $PDSI_{sc} \leq -3$ were approximately twice as likely under 2014 anthropogenic warming levels (Figure S7c). Although uncertainty in probabilities of extreme events is large when based on observed records [e.g., *Swain et al*., 2014], and the anthropogenic trend may not result in a perfectly uniform shift in the $PDSI_{sc}$ distribution, this analysis illustrates the general fact that the anthropogenic drying trend, while still small relative to the range of natural climate variability, has caused previously improbable drought extremes to become substantially more likely, consistent with the conclusions of other recent studies [e.g., *AghaKouchak et al*., 2014; *Cook et al*., 2015; *Diffenbaugh et al*., 2015; *Shukla et al*., 2015; *Williams et al*., 2013, 2014, 2015].

Regarding anthropogenic contributions, there are some important caveats. First, anthropogenic climate change has potentially affected more than just temperature in CA [e.g., *Swain et al*., 2014; *Wang et al*., 2014, 2015]. Lack of long-term observational data on wind speed and humidity in CA, and uncertainties in existing data, make it difficult to quantify anthropogenic influences on these variables. For CA precipitation, current models project a weak overall increase [*Neelin et al*., 2013; *Seager et al*., 2014b, 2015; *Simpson et al*., 2015], but no such precipitation trend has emerged. Hence, we only characterize anthropogenic effects on temperature in this study. Second, observed warming trends are affected by processes not related to greenhouse gas emissions such as land use (e.g., agriculture, urbanization) and natural low-frequency climate variability. While climate models provide a definition of anthropogenic warming that should be unbiased by observations, the accuracy of this approach, as in other attribution studies [e.g., *Bindoff et al*., 2013], is confined by the accuracy of climate models. Finally, our analyses do not account for snowpack, making our results a likely underestimation of the contribution of heat anomalies to recent drought in snow-dominated mountain areas and should be interpreted conservatively regarding the effects of warming on water resources for systems strongly affected by the timing of seasonal runoff from mountains.

4. Conclusions

Anthropogenic warming has intensified the recent drought as part of a chronic drying trend that is becoming increasingly detectable and is projected to continue growing throughout the rest of this century [e.g., *Cook et al*., 2015]. As anthropogenic warming continues, natural climate variability will become increasingly unable to compensate for the drying effect of warming. Instead, the soil moisture conditions associated with the current drought will become increasingly common. Impacts of drought on society may be increasingly intensified due to declining availability of groundwater reserves [e.g., *Famiglietti*, 2014]. The Central Valley may be particularly vulnerable to warming-driven drought if reductions in water supply cause reductions in irrigation, as irrigation has slowed warming in this region [*Lobell and Bonfils*, 2008]. The dramatic effects of the current drought in CA, combined with the knowledge that the background warming-driven drought trend will continue to intensify amidst a high degree of natural climate variability, highlight the critical need for a long-term outlook on drought resilience, even if wet conditions soon end the current drought in CA.

Acknowledgments
We thank Y. Mao for sharing VIC meteorological forcing and soil moisture data from *Mao et al*. [2015]. We thank J. Sheffield for making the SHEFF data set available at http://hydrology.princeton.edu. We thank R. Vose for providing the VOSE data set. PRISM data were obtained from the PRISM Climate Group, Oregon State University (http://www.prism.oregonstate.edu, created 4 February 2004). PRISM dew point data were obtained from http://oldprism.nacse.org. TopoWx data were obtained from ftp://mco.cfc.umt.edu/resources/TopoWx-source/. LDAS data were obtained from http://disc.sci.gsfc.nasa.gov/hydrology/data holdings. GPCC data through 2013 come from ftp://ftp.dwd.de/pub/data/gpcc/html/fulldata_v7_-doi_download.html. PREC/L, NCEP2, NCEP/NCAR, NOAA twentieth century reanalysis, and GPCC for 2014 were accessed from http://www.esrl.noaa.gov. A spatially continuous map of soil moisture holding capacities for the United States came from the Web Soil Survey data set (http://websoilsurvey.nrcs.usda.gov). This work was supported by NSF award AGS-1243204 and NOAA award NA14OAR4310232. Lamont–Doherty publication number 7924. Thanks to K.J. Anchukaitis and two anonymous reviewers for comments that improved this manuscript. The climate and $PDSI_{sc}$ data sets compiled for this study are available at http://www.ldeo.columbia.edu/~williams/ca_drought_2015_grl.html.

The Editor thanks two anonymous reviewers for their assistance in evaluating this paper.

References

Abatzoglou, J. T., D. E. Rupp, and P. W. Mote (2014), Questionable evidence of natural warming of the northwestern United States, *Proc. Natl. Acad. Sci. U.S.A.*, *111*(52), E5605–E5606, doi:10.1073/pnas.1421311112.

AghaKouchak, A., L. Cheng, O. Mazdiyasni, and A. Farahmand (2014), Global warming and changes in risk of concurrent climate extremes: Insights from the 2014 California drought, *Geophys. Res. Lett.*, *41*, 8847–8852, doi:10.1002/2014GL062308.

Berg, N., and A. Hall (2015), Increased interannual precipitation extremes over California under climate change, *J. Clim.*, *28*(16), 6324–6334, doi:10.1175/JCLI-D-14-00624.1.

Bindoff, N. L., et al. (2013), Detection and attribution of climate change: From global to regional, in *Climate Change 2013: The Physical Science Basis. Contribution of Working Group I to the Fifth Assessment Report of the Intergovernmental Panel on Climate Change*, edited by T. F. Stocker et al., pp. 867–952, Cambridge Univ. Press, Cambridge, U. K., and New York.

Cook, B. I., J. E. Smerdon, R. Seager, and S. Coats (2014), Global warming and 21st century drying, *Clim. Dyn.*, *43*(9–10), 2607–2627, doi:10.1007/s00382-014-2075-y.

Cook, B. I., T. R. Ault, and J. E. Smerdon (2015), Unprecedented 21st century drought risk in the American Southwest and Central Plains, *Sci. Adv.*, *1*(1), e1400082, doi:10.1126/sciadv.1400082.

Cook, E. R., C. A. Woodhouse, C. M. Eakin, D. M. Meko, and D. W. Stahle (2004), Long-term aridity changes in the western United States, *Science*, *306*(5698), 1015–1018, doi:10.1126/science.1102586.

Cook, E. R., R. Seager, M. A. Cane, and D. W. Stahle (2007), North American drought: Reconstructions, causes, and consequences, *Earth Sci. Rev.*, *81*(1–2), 93–134, doi:10.1016/j.earscirev.2006.12.002.

Cook, E. R., R. Seager, R. R. Heim Jr., R. S. Vose, C. Herweijer, and C. Woodhouse (2010), Megadroughts in North America: Placing IPCC projections of hydroclimatic change in a long-term palaeoclimate context, *J. Quat. Sci.*, *25*(1), 48–61, doi:10.1002/jqs.1303.

Dai, A. (2011), Characteristics and trends in various forms of the Palmer Drought Severity Index during 1900–2008, *J. Geophys. Res.*, *116*, D12115, doi:10.1029/2010JD015541.

Dai, A., K. E. Trenberth, and T. Qian (2004), A global dataset of Palmer Drought Severity Index for 1870–2002: Relationship with soil moisture and effects of surface warming, *J. Hydrometeorol.*, *5*(6), 1117–1130, doi:10.1175/JHM-386.1.

Daly, C., W. P. Gibson, M. Dogget, J. Smith, and G. Taylor (2004), Up-to-date monthly climate maps for the coterminous United States, paper presented at Proceedings of the 14th AMS Conference on Applied Climatology, 84th AMS Annual Meeting, Am. Meteorol. Soc., Seattle, Washington, 13–16 Jan.

Diaz, H. F., and E. R. Wahl (2015), Recent California water year precipitation deficits: A 440-year perspective, *J. Clim.*, *28*(12), 4637–4652, doi:10.1175/JCLI-D-14-00774.1.

Diffenbaugh, N. S., D. L. Swain, and D. Touma (2015), Anthropogenic warming has increased drought risk in California, *Proc. Natl. Acad. Sci. U.S.A.*, *112*(13), 3931–3936, doi:10.1073/pnas.1422385112.

Famiglietti, J. S. (2014), The global groundwater crisis, *Nat. Clim. Change*, *4*(11), 945–948, doi:10.1038/nclimate2425.

Funk, C., A. Hoell, and D. Stone (2014), Examining the contribution of the observed global warming trend to the California droughts of 2012/13 and 2013/14, in *Explaining Extreme Events of 2013 From a Climate Perspective*, *Bull. Am. Meteorol. Soc.*, edited by S. C. Herring, et al., pp. S11–S15, Am. Meteorol. Soc., Boston, Mass, doi:10.1175/1520-0477-95.9.S1.1.

Griffin, D., and K. J. Anchukaitis (2014), How unusual is the 2012–2014 California drought?, *Geophys. Res. Lett.*, *41*, 9017–9023, doi:10.1002/2014GL062433.

Guttman, N. B. (1998), Comparing the Palmer drought index and the standardized precipitation index, *J. Am. Water Resour. Assoc.*, *34*(1), 113–121, doi:10.1111/j.1752-1688.1998.tb05964.x.

Harter, T., and H. Dahlke (2014), OUTLOOK: Out of sight but not out of mind: California refocuses on groundwater, *Calif. Agric.*, *68*(3), 54–55.

Hartmann, D. L. (2015), Pacific sea surface temperature and the winter of 2014, *Geophys. Res. Lett.*, *42*, 1894–1902, doi:10.1002/2015GL063083.

Heim, R. R., Jr. (2002), A review of twentieth-century drought indices used in the United States, *Bull. Am. Meteorol. Soc.*, *83*(8), 1149–1165, doi:10.1175/1520-0477(2002)083<1149:AROTDI>2.3.CO;2.

Hobbins, M. T., J. A. Ramírez, and T. C. Brown (2004), Trends in pan evaporation and actual evapotranspiration across the conterminous US: Paradoxical or complementary?, *Geophys. Res. Lett.*, *31*, L13503, doi:10.1029/2004GL019846.

Hobbins, M. T., A. Dai, M. L. Roderick, and G. D. Farquhar (2008), Revisiting potential evapotranspiration parameterizations as drivers of long-term water balance trends, *Geophys. Res. Lett.*, *35*, L12403, doi:10.1029/2008GL033840.

Hoerling, M. P., J. K. Eischeid, X.-W. Quan, H. F. Diaz, R. S. Webb, R. M. Dole, and D. R. Easterling (2012), Is a transition to semipermanent drought conditions imminent in the US Great Plains?, *J. Clim.*, *25*(24), 8380–8386, doi:10.1175/JCLI-D-12-00449.1.

Howitt, R., J. Medellin-Azuara, D. MacEwan, J. Lund, and D. A. Sumner (2014), Economic analysis of the 2014 drought for California agriculture, UC Davis Cent. for Watershed Sci., Davis, Calif. [Available at https://watershed.ucdavis.edu/files/biblio/DroughtReport_23July2014_0.pdf.]

Johnstone, J. A., and N. J. Mantua (2014a), Atmospheric controls on northeast Pacific temperature variability and change, 1900–2012, *Proc. Natl. Acad. Sci. U.S.A.*, *111*(40), 14,360–14,365, doi:10.1073/pnas.1318371111.

Johnstone, J. A., and N. J. Mantua (2014b), Reply to Abatzoglou et al.: Atmospheric controls on northwest United States air temperatures, 1948–2012, *Proc. Natl. Acad. Sci. U.S.A.*, *111*(52), E5607–E5608, doi:10.1073/pnas.1421618112.

Liang, X., D. P. Lettenmaier, E. F. Wood, and S. J. Burges (1994), A simple hydrologically based model of land surface water and energy fluxes for general circulation models, *J. Geophys. Res.*, *99*(D7), 14,415–14,428, doi:10.1029/94JD00483.

Lobell, D. B., and C. Bonfils (2008), The effect of irrigation on regional temperatures: A spatial and temporal analysis of trends in California, 1934–2002, *J. Clim.*, *21*(10), 2063–2071, doi:10.1175/2007JCLI1755.1.

Mankin, J. S., and N. S. Diffenbaugh (2015), Influence of temperature and precipitation variability on near-term snow trends, *Clim. Dyn.*, *45*(3–4), 1099–1116, doi:10.1007/s00382-014-2357-4.

Mann, M. E., and P. H. Gleick (2015), Climate change and California drought in the 21st century, *Proc. Natl. Acad. Sci. U.S.A.*, *112*(13), 3858–3859, doi:10.1073/pnas.1503667112.

Mao, Y., B. Nijssen, and D. P. Lettenmaier (2015), Is climate change implicated in the 2013–2014 California drought? A hydrologic perspective, *Geophys. Res. Lett.*, *42*, 2805–2813, doi:10.1002/2015GL063456.

Mitchell, K. E., et al. (2004), The multi-institution North American Land Data Assimilation System (NLDAS): Utilizing multiple GCIP products and partners in a continental distributed hydrological modeling system, *J. Geophys. Res.*, *109*, D07S90, doi:10.1029/2003JD003823.

Monteith, J. L. (1965), Evaporation and environment, *Symp. Soc. Exp. Biol.*, *19*, 205–224.

Moore, J. W., and Z. R. Heath (2015), Forest health protection survey: Aerial detection survey—April 15th–17th, USDA Forest Service, Davis, Calif. [Available at http://www.fs.usda.gov/detail/r5/forest-grasslandhealth/?cid=fsbdev3_046696.]

Mote, P. W. (2006), Climate-driven variability and trends in mountain snowpack in Western North America, *J. Clim.*, *19*(23), 6209–6220, doi:10.1175/JCLI3971.1.

Myhre, G., et al. (2013), Anthropogenic and natural radiative forcing, in *Climate Change 2013: The Physical Science Basis. Contribution of Working Group I to the Fifth Assessment Report of the Intergovernmental Panel on Climate Change*, edited by T. F. Stocker et al., pp. 659–740, Cambridge Univ. Press, Cambridge, U. K., and New York.

Neelin, J. D., B. Langenbrunner, J. E. Meyerson, A. Hall, and N. Berg (2013), California winter precipitation change under global warming in the Coupled Model Intercomparison Project Phase 5 ensemble, *J. Clim.*, *26*(17), 6238–6256, doi:10.1175/JCLI-D-12-00514.1.

Oyler, J. W., A. Ballantyne, K. Jencso, M. Sweet, and S. W. Running (2015), Creating a topoclimatic daily air temperature dataset for the conterminous United States using homogenized station data and remotely sensed land skin temperature, *Int. J. Climatol.*, *35*(9), 2258–2279, doi:10.1002/joc.4127.

Palmer, W. C. (1965), Meteorological drought, 58 pp., U. S. Weather Bur., Washington, D. C. [Available at http://drought.unl.edu/Portals/0/docs/workshops/03222012_Kingston_Jamaica/references/Palmer_PDSIpaper.pdf.]

Penman, H. L. (1948), Natural evaporation from open water, bare soil, and grass, *Proc. R. Soc., Ser. A*, *193*, 120–145.

Pryor, S., and J. Ledolter (2010), Addendum to "Wind speed trends over the contiguous United States", *J. Geophys. Res.*, *115*, D10103, doi:10.1029/2009JD013281.

Pryor, S. C., R. J. Barthelmie, D. T. Young, E. S. Takle, R. W. Arritt, D. Flory, W. J. Gutowski, A. Nunes, and J. Roads (2009), Wind speed trends over the contiguous United States, *J. Geophys. Res.*, *114*, D14105, doi:10.1029/2008JD011416.

Robeson, S. M. (2015), Revisiting the recent California drought as an extreme value, *Geophys. Res. Lett.*, *42*, doi:10.1002/2015GL064593, in press.

Rodell, M., P. R. Houser, U. Jambor, J. Gottschalck, K. Mitchell, C. J. Meng, K. Arsenault, B. Cosgrove, J. Radakovich, and M. Bosilovich (2004), The global land data assimilation system, *Bull. Am. Meteorol. Soc.*, *85*(3), 381–394, doi:10.1175/BAMS-85-3-381.

Roderick, M. L., L. D. Rotstayn, G. D. Farquhar, and M. T. Hobbins (2007), On the attribution of changing pan evaporation, *Geophys. Res. Lett.*, *34*, L17403, doi:10.1029/2007GL031166.

Roderick, M. L., M. T. Hobbins, and G. D. Farquhar (2009), Pan evaporation trends and the terrestrial water balance. II. Energy balance and interpretation, *Geogr. Compass*, *3*(2), 761–780, doi:10.1111/j.1749-8198.2008.00214.x.

Rohde, R., R. A. Muller, R. Jacobsen, E. Muller, S. Perlmutter, A. Rosenfeld, J. Wutele, D. Groom, and C. Wickham (2013), A new estimate of the average Earth surface land temperature spanning 1753 to 2011, *Geoinf. Geostat.*, *1*(1), 1–7, doi:10.4172/2327-4581.1000101.

Scheff, J., and D. M. W. Frierson (2014), Scaling potential evapotranspiration with greenhouse warming, *J. Clim.*, *27*(4), 1539–1558, doi:10.1175/JCLI-D-13-00233.1.

Schneider, U., A. Becker, P. Finger, A. Meyer-Christoffer, M. Ziese, and B. Rudolf (2014), GPCC's new land surface precipitation climatology based on quality-controlled in situ data and its role in quantifying the global water cycle, *Theor. Appl. Climatol.*, *115*(1–2), 15–40, doi:10.1007/s00704-013-0860-x.

Seager, R., M. Hoerling, S. Schubert, H. Wang, B. Lyon, A. Kumar, J. Nakamura, and N. Henderson (2014a), Causes and predictability of the 2011–14 California drought, Natl. Oceanic and Atmos. Admin., Washington, D. C. [Available at http://cpo.noaa.gov/ClimatePrograms/ModelingAnalysisPredictionsandProjections/MAPPTaskForces/DroughtTaskForce/CaliforniaDrought.aspx.]

Seager, R., D. Neelin, I. Simpson, H. Liu, N. Henderson, T. Shaw, Y. Kushnir, M. Ting, and B. Cook (2014b), Dynamical and thermodynamical causes of large-scale changes in the hydrological cycle over North America in response to global warming, *J. Clim.*, *27*(20), 7921–7948, doi:10.1175/JCLI-D-14-00153.1.

Seager, R., M. Hoerling, S. Schubert, H. Wang, B. Lyon, A. Kumar, J. Nakamura, and N. Henderson (2015), Causes of the 2011 to 2014 California drought, *J. Clim.*, doi:10.1175/JCLI-D-14-00860.1, in press.

Sheffield, J., E. F. Wood, and M. L. Roderick (2012), Little change in global drought over the past 60 years, *Nature*, *491*(7424), 435–438, doi:10.1038/nature11575.

Shukla, S., M. Safeeq, A. AghaKouchak, K. Guan, and C. Funk (2015), Temperature impacts on the water year 2014 drought in California, *Geophys. Res. Lett.*, *42*, 4384–4393, doi:10.1002/2015GL063666.

Simpson, I. R., R. Seager, M. Ting, and T. A. Shaw (2015), Causes of change in Northern Hemisphere winter meridional winds and regional hydroclimate, *Nat. Clim. Change*, doi:10.1038/NCLIMATE2783, in press.

Smerdon, J. E., B. I. Cook, E. R. Cook, and R. Seager (2015), Bridging past and future climate across paleoclimatic reconstructions, observations, and models: A hydroclimate case study, *J. Clim.*, *28*(8), 3212–3231, doi:10.1175/JCLI-D-14-00417.1.

Svoboda, M., D. LeComte, M. Hayes, R. Heim, K. Gleason, J. Angel, B. Rippey, R. Tinker, M. Palecki, and D. Stooksbury (2002), The drought monitor, *Bull. Am. Meteorol. Soc.*, *83*(8), 1181–1190, doi:10.1175/1520-0477%282002%29083%3C1181:TDM%3E2.3.CO;2.

Swain, D., M. Tsiang, M. Haughen, D. Singh, A. Charland, B. Rajarthan, and N. Diffenbaugh (2014), The extraordinary California drought of 2013/2014: Character, context and the role of climate change, in *Explaining Extreme Events of 2013 From a Climate Perspective*, *Bull. Am. Meteorol. Soc.*, edited by S. C. Herring, et al., pp. S3–S6, Am. Meteorol. Soc., Boston, Mass., doi:10.1175/1520-0477-95.9.S1.1.

Taylor, K. E., R. J. Stouffer, and G. A. Meehl (2012), An overview of CMIP5 and the experiment design, *Bull. Am. Meteorol. Soc.*, *93*(4), 485–498, doi:10.1175/BAMS-D-11-00094.1.

Thornthwaite, C. W. (1948), An approach toward a rational classification of climate, *Geogr. Rev.*, *38*(1), 55–94, doi:10.2307/210739.

van Vuuren, D. P., et al. (2011), The representative concentration pathways: An overview, *Clim. Change*, *109*(1–2), 5–31, doi:10.1007/s10584-011-0148-z.

Vose, R. S., S. Applequist, M. Squires, I. Durre, M. J. Menne, C. N. Williams Jr., C. Fenimore, K. Gleason, and D. Arndt (2014), Improved historical temperature and precipitation time series for US climate divisions, *J. Appl. Meteorol. Climatol.*, *53*(5), 1232–1251, doi:10.1175/JAMC-D-13-0248.1.

Wang, H., and S. Schubert (2014), Causes of the extreme dry conditions over California during early 2013, in *Explaining Extreme Events of 2013 From a Climate Perspective*, *Bull. Am. Meteorol. Soc.*, edited by S. C. Herring, et al., pp. S7–S10, Am. Meteorol. Soc., Boston, Mass., doi:10.1175/1520-0477-95.9.S1.1.

Wang, S. Y., L. Hipps, R. R. Gillies, and J. H. Yoon (2014), Probable causes of the abnormal ridge accompanying the 2013–2014 California drought: ENSO precursor and anthropogenic warming footprint, *Geophys. Res. Lett.*, *41*, 3220–3226, doi:10.1002/2014GL059748.

Wang, S. Y. S., W. R. Huang, and J. H. Yoon (2015), The North American winter 'dipole' and extremes activity: A CMIP5 assessment, *Atmos. Sci. Lett.*, *16*(3), 338–345, doi:10.1002/asl2.565.

Wells, N., S. Goddard, and M. J. Hayes (2004), A self-calibrating Palmer drought severity index, *J. Clim.*, *17*(12), 2335–2351, doi:10.1175/1520-0442(2004)017<2335:ASPDSI>2.0.CO;2.

Williams, A. P., et al. (2013), Temperature as a potent driver of regional forest drought stress and tree mortality, *Nat. Clim. Change*, *3*(3), 292–297, doi:10.1038/nclimate1693.

Williams, A. P., et al. (2014), Causes and implications of extreme atmospheric moisture demand during the record-breaking 2011 wildfire season in the southwestern United States, *J. Appl. Meteorol. Climatol.*, *53*(12), 2671–2684, doi:10.1175/JAMC-D-14-0053.1.

Williams, A. P., et al. (2015), Correlations between components of the water balance and burned area reveal new insights for predicting fire activity in the southwest US, *Int. J. Wildland Fire*, *24*(1), 14–26, doi:10.1071/WF14023.

Worland, J. (2015), How the California Drought Is Increasing the Potential for Devastating Wildfires, *Time*. [Available at http://time.com/3849320/california-drought-wildfires/.]

Zhao, T., and A. Dai (2015), The magnitude and causes of global drought changes in the 21st century under a low-moderate emissions scenario, *J. Clim.*, *28*(11), 4490–4512.